Científica, vol.19, núm. 2, pp. 75-80, julio-diciembre 2015.
ISSN 1665-0654, ESIME Instituto Politécnico Nacional MÉXICO

Extraction of the Extrinsic Base Resistance of SiGe:C HBTs at 300 K and at 40 K

Eloy **Ramírez-García**
Gonzalo **Pacheco-Álvarez**
Omar **Ramírez-Sampedro**

Instituto Politécnico Nacional,
Escuela Superior de Ingeniería Mecánica y Eléctrica,
Departamento de Telecomunicaciones.
Unidad Profesional "Adolfo López Mateos" Zacatenco,
Col. Lindavista, Del. Gustavo A. Madero, CP 07738,
Ciudad de México.
MÉXICO.

correos electrónicos (email): ramirezg@ipn.mx
gonzalopachecoalvarez@gmail.com
omar_ramirez1890@hotmail.com

Recibido 20-11-2014, aceptado 13-03-2015.

Abstract

This paper introduces the results of the extraction of the extrinsic base resistance reported (R_{Bx}) of a silicon germanium carbon (SiGe:C) heterojunction bipolar transistor (HBT) at room (300 K) and low temperature (40 K). The technique is based on *S*-parameters and electric modeling. In state-of-the-art SiGe:C HBT RBx is the parameter that limits the increase the maximum oscillation frequency (f_{MAX}). Hence a technique that permits the R_{Bx} extraction may be useful to designers to improve f_{MAX} performances, and develop applications in the terahertz regime.

Key words: apparent base resistance, intrinsic base resistance, extrinsic base resistance, heterojunction bipolar transtistors.

Resumen (Extracción de la resistencia de base extrínseca de un transistor bipolar de heterounión SiGe:C a 300K y 40K)

Este documento presenta los resultados de la extracción de la resistencia de base extrínseca (R_{Bx}) de un transistor bipolar de heterounión (TBH) silicio germanio carbono (SiGe:C) a temperatura ambiente (300 K) y a baja temperatura (40 K). La técnica se basa en mediciones de los parámetros S y su modelado eléctrico. En el TBH SiGe:C al estado del arte R_{Bx} es el parámetro que limita el aumento de la frecuencia de oscilación máxima (f_{MAX}). Por lo tanto una técnica que permita la extracción R_{Bx} puede ser útil para los diseñadores para mejorar el rendimiento f_{MAX}, esto con el fin de desarrollar aplicaciones en el régimen de terahertz.

Palabras clave: inteligencia artificial, memorias asociativas, reconocimiento de patrones, memoria de traducción.

1. Introduction

The constant demand for applications with high bandwidth requires improving the dynamic performances of semiconductor devices used in communications equipment. Moreover, nowadays there has been a growing interest in developing low noise amplifiers for terahertz regime [1]. One of the most used semiconductor devices to develop such applications is the silicon germanium carbon (SiGe:C) heterojunction bipolar transistor (TBH), here after these devices will be referred as SiGe HBTs. SiGe HBTs have already demonstrated a maximum oscillation frequency (f_{MAX}) of 500 GHz [2] at room temperature.

Moreover, SiGe HBTs developed using a standard architecture (double poly-silicon/selective epitaxial growth) the f_{MAX} is limited by the extrinsic base resistance (R_{Bx}) [3]. Hence, a proper quantification of the contributions of the apparent base resistance (R_B), $R_B = R_{Bx} + XR_{Bi}$ where R_{Bx} and R_{Bi} are respectively the extrinsic and intrinsic base resistances, and X is the base collector distribution factor [4]. The knowledge of all these parameters should be useful to further improve f_{MAX} and microwave noise (MWN) performances [5].

This work is devoted to describing the extraction strategy of R_{Bx} in advanced SiGe:C HBTs. Section two is devoted to describe SiGe:C devices, section three highlights the static (DC) and dynamic (AC) performances, section four explains the extrinsic base resistance (R_{Bx}) extraction method.

2. Device description and electric model

Measurements are performed between 40 K and 300 K in an open-cycle liquid helium cryostat with *in situ* two movable coplanar probes (IEF-Paris XI). The samples and an impedance standard substrate are in vacuum and they are fixed on the cooled chuck. Probes arms are directly cooled with liquid nitrogen to reduce the heat transfer from the probes to the sample, and to control the thermal gradient along the coaxial waveguides. The *S*-parameters are measured between 50 and 18 GHz at room temperature and at 40 K between 50 MHz and 45 GHz, with a SOLT calibration performed at each temperature. The transistor measurements are "open" de-embedded [6]. The unity current gain frequency (f_T) is extracted with an automatic and robust method described in [7], and f_{MAX} is obtained with a constant value of $(U)^{1/2}$ over the high frequency range, where U is the Mason's gain.

We characterized SiGe HBTs developed by STMicroelectronics. These components are named T1, they have different emitter surface (S_E = 0.13 3.7 or 0.13 5.74 m^2) but the same base parameters: N_{AB} = 3x10^{19} cm^{-3}. We had access to HBTs with two different emitter lengths (and only one emitter width equal to 0.13 µm). Their emitter areas are named S_{E1} = 0.13 3.7 m^2 and S_{E2} = 0.13 5.74 m^2 whit a concentration of Ge = 15-20%. Further details of this HBT technology can be found in [8].

The equivalent electric circuit of the bipolar transistor is a representation of their electrical behavior in the harmonic regime (AC). This circuit consists of a set of two-terminal elements - inductors, abilities, strengths and sources of voltage-controlled current in one of its two possible configurations: *T* or Π. In this work we used the Π configuration, see Fig. 1 (a).

The parameters depicted in figure 1 (a) are the extrinsic base resistance (R_{Bx}), the intrinsic base resistance (R_{Bi}), the distribution factor (X) between the apparent base resistance (R_B) and the base-collector junction capacitance (CBC), and the emitter access resistances (R_E). The extraction of the triplet {R_{Bx}, X, R_{Bi}} will be described in detail later. R_Π, g_m, C_Π and τ_Π have their standard meaning [9]. The value of R_C is equal to 14.5 Ω (for a device with S_{E1}). The method to determine R_C is highlighted in [10] for a SiGe HBT with a collector similar to the devices presented in this work.

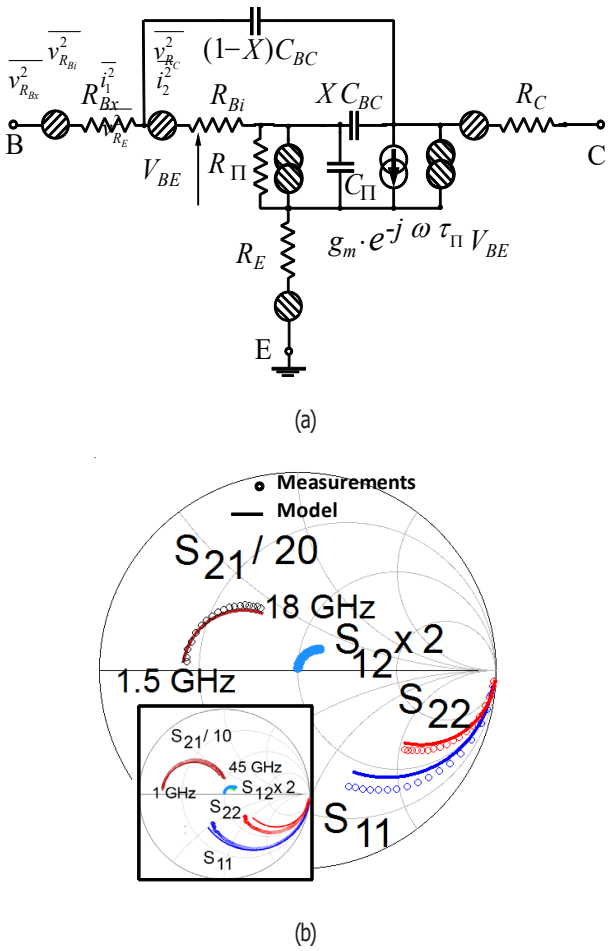

Fig. 1. (a) Π Equivalent circuit of the SiGe HBT. (b) S parameters modelled and measured S parameters at 300 K, J_C = 7.23 mA/ µm^2 and V_{CE} = 1.22 V, at 40 K (inset), J_C = 6.80 mA/ µm^2 and V_{CE} = 1.37 V.

We used an analytical-based method to extract a part of the small-signal parameters. The emitter resistance (R_E) is obtained from the extrapolation of Re(Z_{12}) at infinite emitter current. The apparent base resistance (R_B) can be obtained from Re(Z_{11}-Z_{12}) in the low frequency region of the measurement, and the base-collector capacitance (C_{BC}) is extracted from $I_m(Z_{22}$-$Z_{21})$. Remaining parameters such as the base-emitter (BE) dynamic resistance (R_Π), the BE capacitance (C_Π), the transconductance (g_m), and its high frequency in-excess delay (τ_Π) were determined by error minimization between measured and simulated *S*-parameters [10].

Figure 1 (b) highlights the good agreement between the modeled (continuous lines) and measured (circles) *S*-parameters at both temperatures and at the bias levels described in the caption. We point out that we obtained the same agreement for all bias levels of the characterized devices (at room and 40 K). Finally, these results show that our equivalent circuit extraction procedure is reliable.

3. DC and AC characteristics

We point out that we decided to represent only two temperatures (300 K and 40 K) in figures 2, 3 and 4 for clarity. Moreover for other temperatures our findings concerning DC and AC performances have the same trend as those reported in [12] and references therein.

Fig. 2 introduces the Gummel plot of T1 only at two temperatures at 300 K and at 40 K. The temperature behavior can be described as follows: First, according to the current-voltage dependence, the base-emitter voltage (VBE) should increase at low temperature to have the same collector current density (J_C), because of the reduction in the carrier intrinsic concentration and the increase of the band-gap. From 300 K to 77 K, the intrinsic carrier concentration varies more than 30 orders in magnitude [12]. The device has a good quality in the base emitter junction as demonstrated by the Gummel graphs (Fig. 2 and Fig.3). The range of linearity is observed at low bias voltage (.5V a .8V).

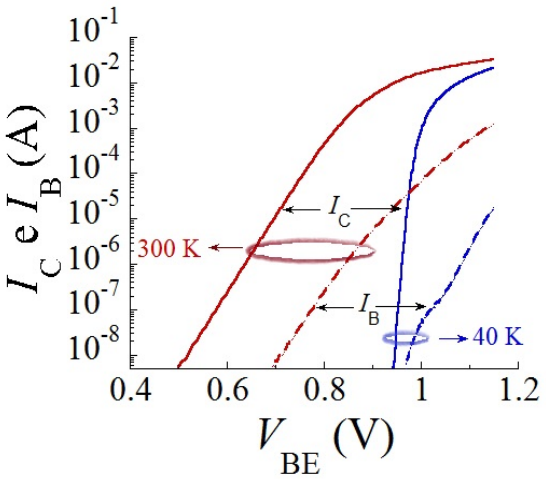

Fig. 2. Gummel plot (I_C and I_B as a function of V_{BE}) at 40 y 300 K.

As shown in Fig. 3, the current gain (β) increase with decreasing temperature because ΔE_V-ΔE_{gE} keeps positive at all temp-eratures. The explanation of the evolution of β as a function of V_{BE} is as follows: Starting from low values of J_C, non- ideal components in the base current lead to the increase of with J_C. The magnitude of the non-ideal current component dominates the low current regime at low temperature and pushes the apparent maximum value of β to higher J_C. From moderate to high J_C, β decreases because of the reverse early effect (base width modulation at the B_E junction). This effect is magnified at low temperature [11]. When V_{BE} or J_C increases the BE space charge region (SCR) is modulated giving a lower effective ΔE_V from base side to emitter side of the SCR which controls hole injection into the emitter. Finally, at high J_C, β collapses because of the apparition of the Kirk effect. Fig. 4 depicts a maximum β of 1900 at room temperature and around 20,000 at 40 K.

Moreover, the current gain has a positive exponential dependence on the reciprocal temperature. This can be expressed as [13]:

$$\beta(T;\Delta E_{gE};\Delta E_{gB}) \propto \exp[(\Delta E_{gB}+\Delta E_V-\Delta E_{gE}/k_BT] \qquad (1)$$

where ΔE_{gB} and ΔE_{gE} are the bandgap narrowing (BGN) of the base and of the emitter, respectively, ΔE_V is the valence band discontinuity at the BE heterojunction, and k_BT is the thermal energy. The conduction band discontinuity is negligible so it can be written $\Delta E_G = \Delta E_V \approx \Delta E_G$ causes the increase of the electron current density at fixed BE voltage.

Fig. 4 depicts the results of the measurements of f_T and f_{MAX} at the two temperatures (300 K and 40 K).

To describe the behavior of f_T as a function of I_C, we will use the following formula:

$$f_T \approx \frac{1}{2\pi\tau_{BC}} = \frac{1}{2\pi(\tau_E+\tau_C+\tau_B+r_E(C_{BE}+C_{BC})+(R_E+R_C)C_{BC})} \qquad (2)$$

where $r_E(C_{BE}+C_{BC})$, with $r_E \approx k_BT/qI_E$, is the charging time of the base-emitter junction, τ_B and τ_C are, respectively, the transit time of the base, and collector; all the other parameters have been already defined.

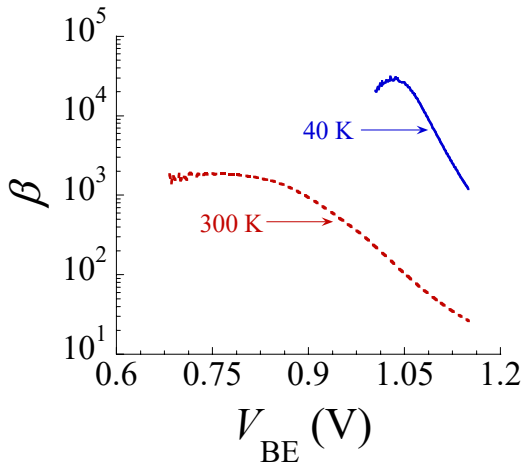

Fig. 3. DC current gain (β), Ge = 15-20%, N_{AB} = 2.5 1019 cm^{-3} at 40 K (continuous line) and 300 K (discontinuous line).

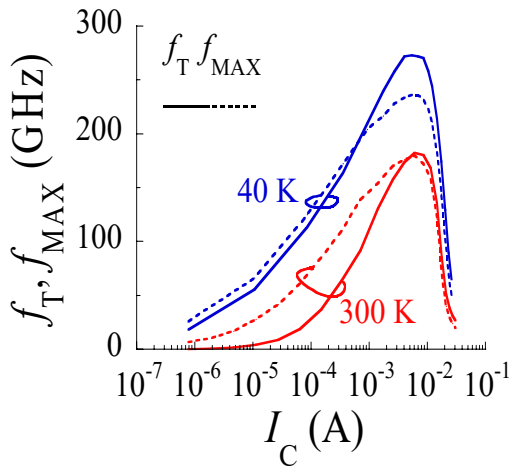

Fig. 4. Transition frequencies (f_T and f_{MAX}) at 300 K and 40 K as a function of collector current (I_C).

As highlighted by relation (2), and at fixed temperature, f_T increases with I_C because the term $r_E(C_{BE} + C_{BC})$ decreases as I_C progresses ($I_C \approx I_E$, if $\beta >> 1$). In fact, time within the SiGe HBTs and at low polarization $r_E(C_{BE} + C_{BC})$ is the highest dominating delay time.

At low temperatures, and at affixed I_C,f_T increases because τ_B and τ_C and the charging time $(R_C + R_C)C_{BC}$ improve. τ_B and τ_C improve because the interaction carrier-phonon decrease and because the carrier saturation velocity increases at low temperature [14] and references therein. $(R_C + R_E)C_{BC}$ improve because at low temperature the better carrier dynamics diminishes the access resistances R_C and R_E (around 15%), and because CBC improves by 12% when T decreases from 300 K to 40 K. All these reasons explain the better f_T performances at 40 K.

Figure 4 shows that f_{MAX} improves as a function of I_C up to the apparition of high level injection phenomena such as the Kirk effect. To understand this trend we will use the following relation of f_{MAX}.

$$f_{MAX} = \sqrt{\frac{f_T}{8\pi R_B C_{BC}}} \qquad (3)$$

where most parameters have been already defined.

As demonstrated by (3) the squared of f_{MAX} is directly proportional to f_T. Hence, at fixed temperature, f_{MAX} improves with I_C because the diminution of the charging time $r_E(C_{BC}+ C_{BC})$.

At fixed I_C,f_{MAX} improve with decreasing temperature because of the f_T improvement and because the term $R_C C_{BC}$ also decreases with T, for the reasons already described.

4. Apparent base resistance elements separation

The factors affecting the access resistances of the bipolar devices are temperature (if the temperature decreases improve access resistances), the geometry of the device (the larger the emitter surface is, the lower the parasitic resistances are).

However, in the literature on the subject never a quantitative mention of how these factors (temperature and geometry) affects access resistances of bipolar components. In this section we will introduce some results of the extraction of extrinsic base resistances and the impact of temperature on their amplitudes.

The apparent base resistance (R_B) is obtained from measured S parameters from which we can obtain Z parameters:

$$R_B = \mathrm{Re}(Z_{11} - Z_{12})|_{1f} = R_{Bx} + XR_{Bi} \qquad (4)$$

where "lf" stands for low frequency (f < 5 GHz) [5].

Once R_B is known this can be plotted in inverse function of the collector model (I_C). R_{Bx} is extracted from a linear regression and then extrapolating R_B to $1/I_C \rightarrow 0$. Fig. 5 summarizes this process. This R_{Bx} extraction strategy is possible because R_{Bx} is independent of I_C [4].

Table 1 reports the results of the extraction of R_{Bx} of the two HBTs varying in emitter surface (S_E) and at two temperatures. These results were extracted using the method already described.

Results introduced by table 1 show that R_{Bx} is inversely proportional to the length of the transistor emitter L_E–here L_E = 3.7 µm for R_{Bx21} or 5.74 µm for R_{Bx23}–, hence $L_{E2}/L_{E21} = 1.55$. Please note that from the results reported in Fig. 5 $R_{Bx21}/R_{Bx23} = 1.58 \approx L_{E23}/L_{E21}$ at 300 K, and $R_{Bx21}/R_{Bx23} = 1.68$ at 40 K.

These results demonstrate that the extraction methodology is proper because the results of R_{Bx21} and R_{Bx23} follow the scaling of L_E.

5. Conclusions

This paper presented a reliable technique for the separation of the extrinsic base resistance, R_{Bx}, and we demonstrate that this technique is valid at room and low temperatures (300 K and 40 K). This extraction avoids the usage of geometric criteria to extract R_{Bx}. This method is based on the use of S-parameter measurements at low frequency range (f < 5 GHz) and electrical modeling. The results demonstrated that R_{Bx} scales with the emitter length (LE) at 300 K and at 40 K.

A remarkable feature is that, to the authors' knowledge, this is the first time that R_{Bx} is obtained at two different temperatures (300 K and 40 K) for advanced SiGe:C HBTs.

Finally, this technique may be useful to designers to improve dynamic performances of f_{MAX} of state-of-the-art SiGe:C HBTs.

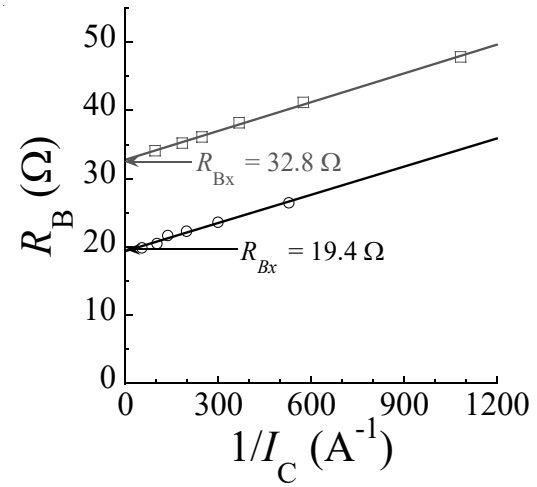

Fig. 5. Apparent base resistance (R_B) as a function of the inverse of the collector current ($1/I_C$) at 40 K and for two emitter surfaces: S_{E21} = 0.17 x 3.7 m^2 (R_{Bx21}) and S_{E21} = 0.17 x 5.74 m^2 (R_{Bx23}).

Tabla 1. Extracted extrinsic base resistance (R_{Bx}) at two temperatures, device T1 and for two emitter surfaces: S_{E21} = 0.17×3.7 m^2 (R_{Bx21}) and S_{E21} = 0.17×5.74 m^2 (R_{Bx23}).

Element	300 K	40 K
R_{Bx21}	32.6	20.6
R_{Bx23}	32.8	19.4

Aknowledgments

Authors would like to thank STMicroelectronics and A. Chantre for providing the devices

References

[1] D Russel, et al. Low-Power Very Low-Noise Cryogenic SiGe IF Amplifiers for Terahertz Mixer Receivers. *IEEE Microwave Theory and Tech*., 60, pp 1641-1648, 2012.

[2] B. Heinemann et al. SiGe HBT Technology with f_T/f_{Max} of 300GHz/500GHz and 2.0 ps CML Gate Delay. *Proc. of the Int. Electron Dev. Meet*., pp 30.5.1-4, Dec. 2010.

[3] E. Canderle et al. Extrinsic base resistance optimization in DPSA-SEG SiGe:C HBTs. Proc. BiCMOS, pp. 1-4, 2012.

[4] N. Zeronian, F. Aniel, M. Riet, B. Barbalat, P. Chevalier, A Chantre. Parasitic electrostatic capacitance of high-speed SiGe Heterojunction bipolar transistors. *Solid State Elec.,* 53, pp.483-489,2009.

[5] E. Ramirez-Garcia et al. Germanium content and base doping level influence on extrinsic base resistance and dynamic performances of SiGe:C heterojunction bipolar transistors. *Semicond. Science and Tech.,* 29, 095020, 2014.

[6] P.J. Van Wijnen, H.R. Claessen, E.A. Wolsheimer. A new straight forward calibration and correction procedure for "On wafer" high frequency S-parameters measurements (45 MHz - 18 GHz). Presented at *IEEE International Electron Devices Meeting* 1989. p. 70-73.

[7] N. Zerounian, F Aniel, R Adde. Complex current gain and cutoff frequency determination of HBTs. *IEE Electronics Letters* 2000; 36:1236-37.

[8] P. Chevalier et al. 230-GHz Self-Aligned SiGeC HBT for Optical and Millimeter-Wave Applications. *J. of Solid-State Circts*, 40, pp. 2025-2034, 2005.

[9] A. Oudir et al. Direct Extraction Method of HBT Equivalent-Circuit Elements Relying Exclusively on S-Parameters Measured at Normal Bias Conditions. *(IEEE) Trans. Microw. Theory and Tech*., 59, 1973-1982, 2011.

[10] E. Ramirez-Garcia et al. SiGe:C HBT transit time analysis based on hydrodynamic modeling using doping, composition and strained dependent SiGe:C carriers mobility and relaxation time. *Solid-State Electron*. 61, pp. 58-64, 2011.

[11] D.M. Richey, et al. Evidence for non equilibrium base transport in Si and SiGe bipolar transistors at cryogenic temperatures." *Solid State Electron*., 39, 785-789, 1996.

[12] J.D. Cressler, et al. On the profile Design and Optimization of Epitaxial Si and SiGe-base bipolar technology for 77 K applications. Part I. *(IEEE) Trans. Electron Dev*, 40, pp 525-541, 1993.

[13] J.D. Cressler, JH Comfort, EF Crabbé, GL Patton, JMC Stork. On the profile design and optimization of epitaxial Si-and SiGe-base bipolar technology for 77 K applications. Part I. *IEEE Trans Electron Dev*, pp 525-41 , 1993.

[14] E. Ramírez-Garcia. Análisis experimentas y modelado de ruido de de alta frecuencia en tansistores bipolares de heterounion (TBH) para Aplicaciones en Telecomunicaciones, Tesis de Doctorado, Instituto Politécnico Nacional, pp. 70-74, 2012.